Electronic Supplementary Information for:

Energy bands matched photocatalysis enhancement based on viologen derivatives electron-transfer- mediator

Fang Niu,[a] Jia-Lin Zhu, [a] Yong Ding, [a] Li-Ming Tao [b] and Jun Jin[a]**

[a] Key Laboratory of Advanced Catalysis of Gansu Province, College of Chemistry and Chemical Engineering, Lanzhou University, Lanzhou, Gansu 730000, China.

[b] Key Laboratory of Science and Technology on Wear and Protection of Materials, Lanzhou Institute of Chemical Physics, Chinese Academy of Sciences, Lanzhou, Gansu 730000, China.

Email addresses: taolm@licp.cas.cn (Li-Ming Tao), jinjun@lzu.edu.cn (Jun Jin)

Table of Contents

1. General methods

1.1 Materials.

Terephthalonitrile, Trifluoromethanesulfonic acid, 4,4-Bipyridine, 4-Bromomethylbenzoic acid , Benzyl bromide, 1-Chloro-2,4-dinitrobenzene, Aniline, and 4-Aminophenol were purchased from Anhui Zesheng Technology Co., Ltd and used as received without further purification. Acetonitrile, ethanol, concentrated sulfuric acid (98 wt.%), D_2O, tetrahydrofuran and ethyl ether were purchased from China National Pharmaceutical Group Corporation and used as received without further purification.

1.2 Characterization methods.

The as-synthesized CTF and o-CTF were conducted the basic characterization to confirm the successful synthesis. X-ray diffraction (XRD) was recorded on a Smartlab SE X-ray diffractometer. Cu K_α as the radiation (λ=0.154 nm) and the radiation entrance slit width was 1 mm. Both CTF and o-CTF were observed using a continuous 2θ scan from 2.0 – 60º (Omega = 1.0º). X-ray photoelectron spectroscopy (XPS) was recorded on a thermo scientific NEXSA X-ray photoelectron spectrometer. Infrared spectra were recorded on a BRUKER V70 fourier transform infrared spectrometer. KBr tablet pressing method was employed to collect the IR spectra. TEM images were got from a Tecnai F30 transmission electron microscope. SEM images were got from a Hitachi S-4800 scanning electron microscope. The working distance was 10 mm and the accelerating voltage was 5 kV. Combustion elemental analysis was conducted on Vario EL III Elemental Analyzer System. UV-Vis spectra were recorded on a UV-2550 UV spectrophotometer. NMR ^1H spectra were measured on Bruker 400MHz superconducting NMR spectrometer (AVANCE III HD 400MHz). A CHI 660E electrochemical workstation was used to record the linear voltammetry curves, voltammetry curves, photocurrent curves, electrochemical impedance spectroscopy and Mott-Schottky plots. Fluorescence spectrum and fluorescence lifetime plots were recorded on a steady-state and time-resolved fluorescence spectrofluorometer (FLS 920).

2. Synthesis of samples and viologen derivatives.

2.1 Synthesis of CTF.

Scheme S1 illustrated the reaction process during keeping at 200 °C for 48h of the reaction mixture. The terephthalonitrile was constructed to covalent triazine frameworks (CTF) through –CN polymerizing to a triazine ring and this conclusion has been confirmed by the basic characterization. Actually, the similar synthesis procedure has been reported[S1] and our sample was prepared according to the reported method with slight modification.

2.2 Synthesis of CBV.

1,1'-bis(4-carboxybenzyl)-[4,4'-bipyridine]-1,1'-diium bromide (CBV) was prepared following the reported method[S2]. Typically, 78.1 mg (0.5 mmol) of 4,4 '- bipyridine and 215 mg (1 mmol) of 4-bromomethylbenzoic acid were dissolved in 100 ml of acetonitrile. The mixture was then refluxed and stirred at 90 °C for 12h to give light green precipitate. The light green precipitate was filtered and washed with acetonitrile (4 × 50 mL). Then it was dried in vacuum for 12h to give 264.1 mg CBV product and the yield was 90.1%.

^{1}H NMR (D_2O, 400 MHz): δ (ppm) 9.09-9.08 (d, 4H), 8.46-8.45 (d, 4H), 7.99-7.97 (d, 4H), 7.50-7.48 (d, 4H), 5.92 (s, 4H).

2.3 Synthesis of DBV.

1,1'-dibenzyl-[4,4'-bipyridine]-1,1'-diium bromide (DBV) was also prepared following the reported method [S2]. Typically, 78.1 mg (0.5 mmol) of 4,4 '-bipyridine and 118 μL (171 mg, 1 mmol) of benzyl bromide were dissolved into 100 ml of acetonitrile. The reaction mixture was then refluxed and stirred at 90 ° C for 12h to give light yellow precipitate. The resulting light yellow precipitate was filtered and washed with acetonitrile (4 × 50 mL). The light yellow precipitate was subsequently dried under vacuum for 12h to yield 221mg DBV product and the yield was 88.7%.

^{1}H NMR (D_2O, 400 MHz): δ (ppm) 9.06-9.04 (d, 4H), 8.43-8.41 (d, 4H), 7.43 (s, 10H), 5.83 (s, 4H).

2.4 Synthesis of DPV.

1,1'-bis(4-hydroxyphenyl)-[4,4'-bipyridine]-1,1'-diium chloride (DPV) was prepared

following the reported method[S3]. In a typical procedure, 312.4 mg (2 mmol) of 4,4 '-bipyridine and 810.2 mg (4 mmol) of 1-chloro-2,4-dinitrobenzene were dissolved into 100ml of acetonitrile. The reaction mixture was then refluxed and stirred at 90 °C for 5 days. After that, the reaction suspension was filtered and washed with acetonitrile (4 × 50 mL) to give white powder. The as-obtained white powder was then dried under vacuum for 12h to give 898mg (yield, 80%) of 1,1'-bis(2,4-dinitrophenyl)-[4,4'-bipyridine]-1,1'-diium chloride (7). Immediately, 280.7 mg (0.5 mmol) of 1,1'-bis(2,4-dinitrophenyl)-[4,4'-bipyridine]-1,1'-diium chloride (7) and 91 μL (93.1 mg, 1 mmol) of aniline were dissolved into 50 mL of ethanol. The reaction mixture was then refluxed and stirred at 78 °C for 7 days. After cooling down to room temperature, the reaction mixture was poured into 250 mL THF. After 6h of placement, the resulting yellowish brown precipitation was filtrated and washed with THF (4 × 50 mL) and ether (2 × 50 mL) sequentially. The as-obtained yellowish brown powder was then dried under vacuum for 12h to yield 265.5 mg (yield, 70%) of 1,1'-diphenyl-[4,4'-bipyridine]-1,1'-diium chloride.

^{1}H NMR (D_2O, 400 MHz): δ (ppm) 9.34-9.32 (d, 4H), 8.72-8.70 (d, 4H), 7.76-7.67 (m, 10H).

2.5 Synthesis of HPV.

1,1'-bis(4-carboxybenzyl)-[4,4'-bipyridine]-1,1'-diium chloride (HPV) was prepared following the reported method [S3]. The synthesis of 1,1 '- bis (2,4-dinitrophenyl) - 4,4' - bipyridine dichloride (7) was the same as above mention. For 1,1'-bis(4-hydroxyphenyl)-[4,4'-bipyridine]-1,1'-diium chloride (HPV) preparation, 280.7 mg (0.5 mmol) of 1,1 '- bis (2,4-dinitrophenyl) - 4,4' - bipyridine dichloride (7) and 109.1 mg (1 mmol) of 4-aminophenol were dissolved into 50 mL of ethanol. The reaction mixture was then stirred and refluxed at 78 °C for 7 days. After that, the solution was cooled down to room temperature and was poured into 250 mL THF. After 6 hours placement, purple precipitate emerged. The resulting purple precipitate was filtrated and washed with THF (4 × 50 mL) and ether (2 × 50 mL) sequentially. The as-obtained purple powder was then dried under vacuum for 12h to give 273 mg of HPV sample with a yield of 67%.

^{1}H NMR (D_2O, 400 MHz): δ (ppm) 9.24-9.22 (d, 4H), 8.64-8.63 (d, 4H), 7.63-7.60 (d, 4H), 7.10-7.08 (d, 4H).

3. Photocatalysis experiment and photocatalytic-related measurement.

3.1 Photocatalysis test.

3.1.1 Photocatalytic oxygen evolution test.

In the photocatalytic oxygen evolution experiment, for more accurate measurement, a sealed container with smaller volume (100 mL) was used due to the less amount of oxygen evolution compared to hydrogen evolution. The light source, irradiation intensity and efficient irradiation area were kept the same as hydrogen evolution. The amount of oxygen evolution was also measured using a gas chromatography (Techcomp GC7900, N_2 carrier) with a TCD detector. The reaction temperature control and the air removal procedure were the same as hydrogen evolution process. In a typical procedure, 10 mg o-CTF was dispersed into 10 mL deionized water. Then 1.5 mg $Co(NO_3)_2$ (3 wt.% Co^{2+}) and 16.9 mg $AgNO_3$ was added into the water suspension to acted as the co-catalyst and sacrificial reagent, respectively. For photocatalytic enhancement measurement, 2 wt.% CBV was also added into the reaction mixture.

3.1.2 Overall water splitting test.

For overall water splitting, 10 mg o-CTF was dispersed into 10 mL deionized water and 1 wt.% Pt (as co-catalyst) was deposited onto o-CTF by in-situ photodeposition. The generated H_2 and O_2 was measured by GC. Other reaction conditions were the same as oxygen evolution experiment. For photocatalytic enhancement measurement, 2 wt.% CBV was also added into the reaction mixture.

3.2 The AQE measurement.

The apparent quantum efficiency (AQE) for hydrogen evolution was measured under the same reaction condition expect for the Xenon lamp was equipped with different band-pass filters, including 420, 450, 500, 550 and 650 nm.

The AQE was calculated as follow:

$$\eta_{AQE} = \frac{N_{electron}}{N_{photon}} \times 100\% = \frac{2 \times n_{H_2} \times N_A}{N_{photon}} \times 100\% = \frac{2 \times n_{H_2} \times N_A}{\frac{E_{total}}{E_{photon}}} \times 100\%$$

$$= \frac{2 \times n_{H_2} \times N_A}{\frac{S \times P \times t}{h \times \frac{c}{\lambda}}} \times 100\% = \frac{2 \times n_{H_2} \times N_A \times h \times c}{S \times P \times t \times \lambda} \times 100\%$$

Where $N_{electron}$ is the number of transferred electrons, N_{photon} is the number of incident photons, N_A is Avogadro constant (6.022×10^{23} mol^{-1}), n_{H_2} is number of H_2 moles and two electrons need to be transferred for every H_2 produced, E_{total} is the total enery of incident light, E_{photon} is the enery of a single photon, S is the efficient irradiation area (3.74 cm^2), P is the intensity of irradiation light and it is different under different band-pass filters, t is the time (s) of photo reaction, h is the Planck constant (6.626×10^{-34} J. s), c is the speed of light (3×10^8 m. s^{-1}), λ is the wavelength (m) of the monochromatic light.

For AQE measurement in every experiment, five values that under the five different band-pass filters (420 nm, 450 nm, 500 nm, 550 nm and 650nm) were obtained. The average hydrogen amounts that produced in the photocatalytic reaction for 1 h was taken to calculate AQE.

3.3 Photoelectrochemical measurement.

The photoelectrochemical measurement was carried out in an electrochemical cell with a flat quartz window. Generally, 5 mg of photocatalyst was dispersed into 1 mL ethanol to form a suspension. An ITO glass was pre-cleaned with water and ethanol for three times and dried in air. Then, 100 μL photocatalyst suspension was drop-coated on the clean ITO surface to form a thin film with certain area (1 cm × 1 cm). Then the three electrodes system was used to measure on CHI 660D electrochemical workstation, where the photocatalyst-coated ITO glass acted as the working electrode, a Pt plate acted as the counter electrode and Hg/Hg_2Cl_2 (SCE) acted as the reference electrode. A 0.2 $mol \cdot L^{-1}$ Na_2SO_4 (pH = 6.8) solution was used as electrolyte solution. A 300 W Xenon lamp with was used as the light source during the measurement. In

control experiment, 1 wt.% Pt was deposited on the photocatalyst and certain amount viologen derivatives was added into the 0.2 mol·L^{-1} Na_2SO_4 (pH = 6.8) electrolyte. Exactly, we prepared a series of solutions that contained 0.1 wt.% CBV, 0.2 wt.% CBV, 0.5 wt.% CBV, 1 wt.% CBV, 2 wt.% CBV, 3 wt.% CBV, 2 wt.% DBV, 2 wt.% DPV or 2 wt.% HPV in 0.2 mol·L^{-1} Na_2SO_4 (pH = 6.8) electrolyte, respectively. The working electrodes with photocatalyst-coated ITOs were firstly immersed into the above electrolytes for 1 minute before photoelectrochemical measurement. The mass concentrations of viologen derivatives in 0.2 mol·L^{-1} Na_2SO_4 solution were kept the same as the concentration in photocatalytic reactions. While in photocatalytic reaction, the mass concentrations of viologen derivatives referred to the mass ratio of the viologen derivatives to the photocatalyst. Take 2 wt.% CBV for example, in photocatalytic reaction, 10 mL deionized water and 10 mg photocatalyst was mixed together, then 0.2 mg CBV is needed to obtain a 2 wt.% CBV solution. While in the photoelectrochemical experiment, 50 mL 0.2 mol·L^{-1} Na_2SO_4 solution was prepared, then 1 mg CBV is needed to obtain a 2 wt.% CBV solution.

3.3.1 LSV measurement.

The linear voltammetry is firstly carried out to study the hydrogen evolution potentials in the above electrolyte solutions. The working electrode is photocatalyst-coated ITO glass and 1 wt.% Pt is deposited on the photocatalyst. The potential range is from 0.242 V to -0.758 V with a scan rate of 50 mV· s^{-1}. The potential is the value versus standard hydrogen electrode (SHE).

3.3.2 I-t measurement.

According to the LSV results, we fixed -0.7 V (vs. SHE) as the target potential to measure I-t curves. We recorded a series of I-t curves at -0.7 V (vs. SHE) in the above electrolyte solutions using three-electrode system. The photocatalyst-coated ITO glass was working electrode, Pt plate was counter electrode and Hg/Hg_2Cl_2 (SCE) was the reference electrode. Xenon lamp was the light source and illuminated the ITO glass from the back side. The on/off photocurrent response was recorded at each 200 seconds.

3.3.3 Electrochemical impedance spectroscopy (EIS) measurement.

Electrochemical impedance spectra (EIS) was also measured under the frequency range of 5 mHz to 100 kHz with 10 mV amplitude. We recorded a series of Nyquist curves in the above electrolyte solutions using three-electrode system. The photocatalyst-coated ITO glass was working electrode, Pt plate was counter electrode and Hg/Hg_2Cl_2 (SCE) was the reference electrode. Xenon lamp was the light source and illuminated the ITO glass from the back side.

3.3.4 Mott-Schottky measurement.

Mott-Schottky curves were performed in the dark at 1 V ~ -1V (vs. SHE) with an amplitude of 5 mV and frequencies of 1000, 1500 and 2000 Hz. The electrolyte was 0.2 $mol \cdot L^{-1}$ Na_2SO_4 solution without any viologen derivatives added. The photocatalyst-coated ITO glass was working electrode, Pt plate was counter electrode and Hg/Hg_2Cl_2 (SCE) was the reference electrode. The photocatalyst were o-CTF and CTF without any Pt deposition.

3.4 Electron-transfer constant (k_{ET}) measurements.

The electron-transfer constants k_{ET} were determined by the peak current linear fitting using the Nicholson method[S4]:

$$i_p = 2.69 \times 10^5 n^{\frac{3}{2}} D^{\frac{1}{2}} \upsilon^{\frac{1}{2}} Ac$$

Where n is number of transferred electrons, D is diffusion coefficient, υ is scanning speed, A is electrode area, c is concentration of substances involved in electrode reaction. In our experiment, the glassy carbon electrode was used and the area A = 0.07 cm^2. The DMSO solution containing 0.05 mol L^{-1} tetrabutylammonium hexafluorophosphate was used as the supporting electrolyte. The concentration for CBV, DBV, DPV and HPV were all kept at 1×10^{-6} mol cm^{-3} in DMSO solution.

The k_{ET} was calculated using the following equation:

$$k_{ET} = \Psi(\pi AD)^{\frac{1}{2}}$$

Where D can be calculated from the slope of: $i_p \sim \upsilon^{\frac{1}{2}}$, and Ψ can be calculated from the Nicholson method for CV. After that, electron-transfer constant k_{ET} was evaluated by the Nicholson's formula.

All of the fitted slope of $i_p \sim \upsilon^{\frac{1}{2}}$ curves, the calculated $D^{1/2}$ from the slope of $i_p \sim \upsilon^{\frac{1}{2}}$, the estimated Ψ from the Nicholson method for CV and the evaluated electron-transfer constant k_{ET} had been listed in Table S5.

3.5 Time-correlated single photon counting (TCSPC) measurements.

For time-correlated single photon counting measurement, five o-CTF samples, including o-CTF+1%Pt, o-CTF+1%Pt+2%CBV, o-CTF+1%Pt+2%DBV, o-CTF+1%Pt+2%DPV, o-CTF+1%Pt+2%HPV, were prepared. For preparation o-CTF+1%Pt+2%CBV sample, 10 mg o-CTF was dispersed in 10 mL deionized water, then 1 mL triethanolamine and 0.21 mg H_2PtCl_6 were added into the reaction mixture to in-situ photo deposit 1 wt.% Pt on the o-CTF. The photodeposition process was carried out under Xenon lamp irradiation for 1h at room temperature. After that, the o-CTF+1%Pt sample was filtered, washed with water, and redispersed into 1 mL ethanol. Then, 0.2 mg CBV was mixed with this suspension and vapored at 60 °C to yield o-CTF+1%Pt+2%CBV sample. The procedures for other samples preparation were the similar to o-CTF+1%Pt+2%CBV sample, except for the different viologen derivatives were added.

The time-correlated single photon counting measurement was then carried out on a steady-state and time-resolved fluorescence spectrofluorometer (FLS 920). Decay times were fitted by Exp. Reconvolution Fit using the suggested lifetime estimates. The fitting equation was as follow:

$$\mathbf{Counts} = \mathbf{A} + \mathbf{B_1} \cdot \mathbf{e}^{\left(-\frac{t}{\tau_1}\right)} + \mathbf{B_2} \cdot \mathbf{e}^{\left(-\frac{t}{\tau_2}\right)} + \mathbf{B_3} \cdot \mathbf{e}^{\left(-\frac{t}{\tau_3}\right)}$$

The fitted parameters had been listed in Table S1.

The average fluorescence decay life was calculated according to the following equation:

$$\bar{\tau} = \frac{\mathbf{B_1\tau_1^2} + \mathbf{B_2\tau_2^2} + \mathbf{B_3\tau_3^2}}{\mathbf{B_1\tau_1} + \mathbf{B_2\tau_2} + \mathbf{B_3\tau_3}}$$

3.6 UV-Vis DRS measurements.

For UV–Visible diffuse reflectance spectrum (DRS) measurement, several powder samples were prepared. Typically, o-CTF+1%Pt, o-CTF+1%Pt+2%CBV, o-CTF+1%Pt+2%DBV, o-CTF+1%Pt+2%DPV and o-CTF+1%Pt+2%HPV were prepared using the same procedure as that for TCSPC measurement. $BaSO_4$ was used as reference. The UV-Vis diffuse reflectance spectra were recorded on a UV-2550 UV spectrophotometer equipped with an integrating ball attachment.

3.7 DFT calculation.

For finding the molecular orbital energy levels, four viologen derivatives, including 1,1'-bis(4-carboxybenzyl)-[4,4'-bipyridine]-1,1'-diium bromide (CBV), 1,1'-dibenzyl-[4,4'-bipyridine]-1,1'-diium bromide (DBV), 1,1'-diphenyl-[4,4'-bipyridine]-1,1'-diium chloride (DPV) and 1,1'-bis(4-hydroxyphenyl)-[4,4'-bipyridine]-1,1'-diium chloride (HPV), as well as a CTF model molecular and a o-CTF model molecular were carried out DFT calculation in Gaussian 09w software package. The ground-state geometry optimization was carried out with B3LYP function and 6-31G+ (d) basis set.

4. Supplementary figures and tables

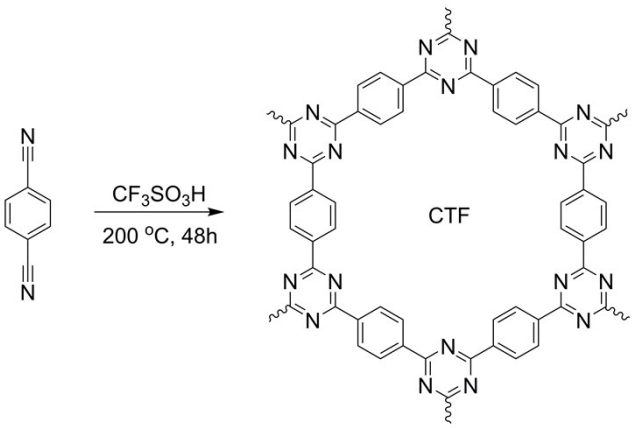

Scheme S1. The synthesis of CTF.

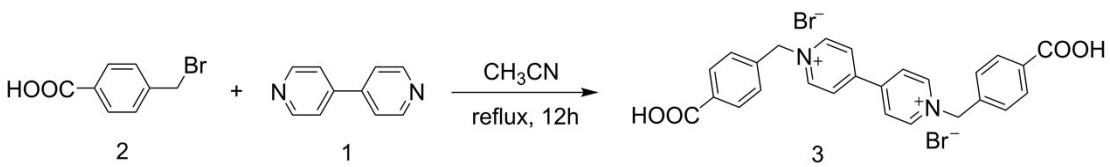

2 1 3

Scheme S2. Synthetic pathway for CBV (3).

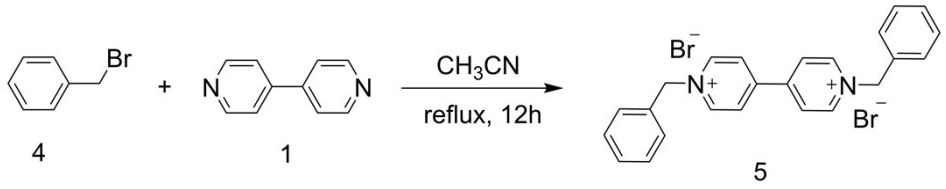

4 1 5

Scheme S3. Synthetic pathway for DBV (5).

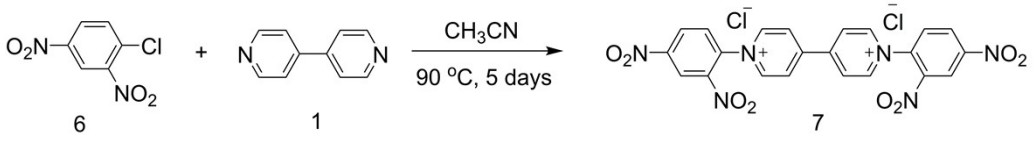

6 1 7

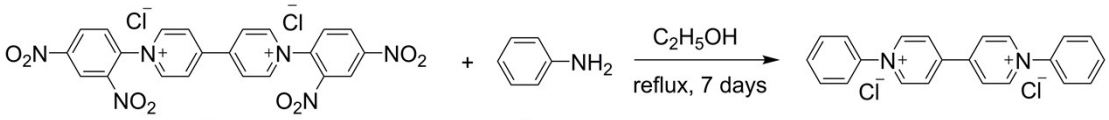

7 8 9

Scheme S4. Synthetic pathway for DPV (9).

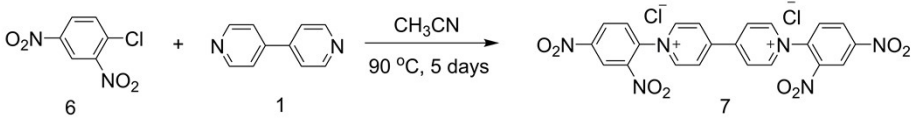

6 1 7

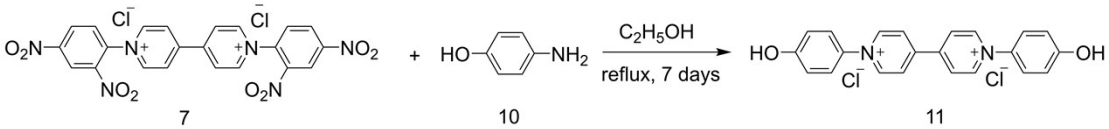

7 10 11

Scheme S5. Synthetic pathway for HPV (11).

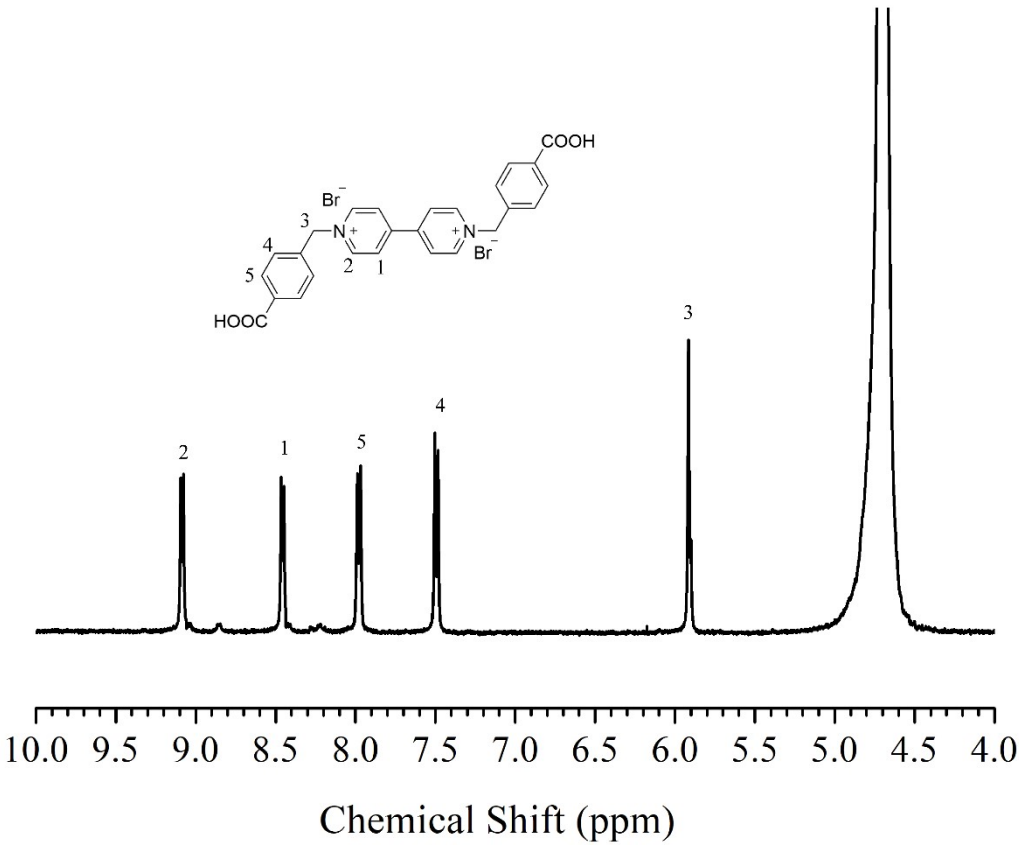

Fig. S1. [1]H NMR spectrum of CBV.

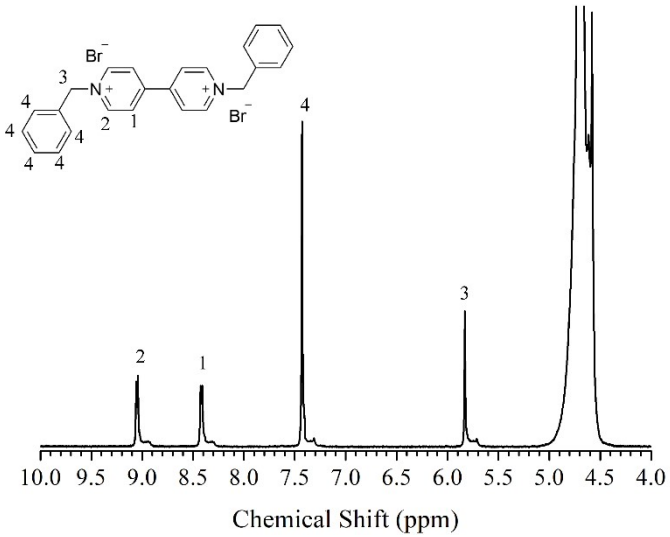

Fig. S2. 1H NMR spectrum of DBV.

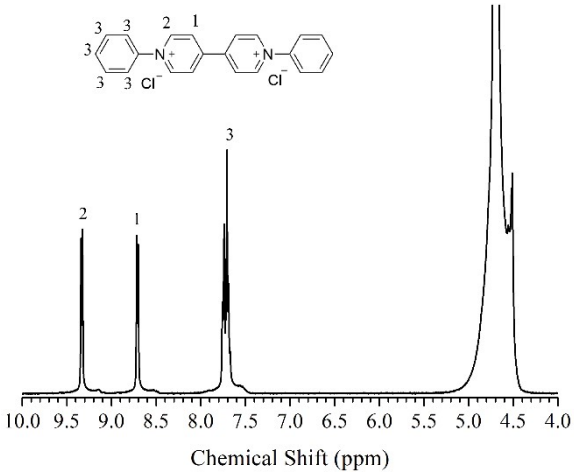

Fig. S3. ^{1}H NMR spectrum of DPV.

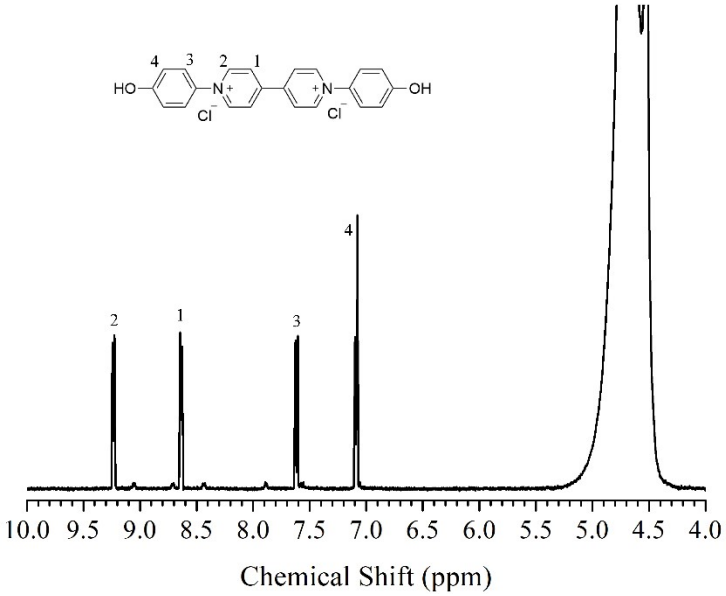

Fig. S4. ^{1}H NMR spectrum of HPV.

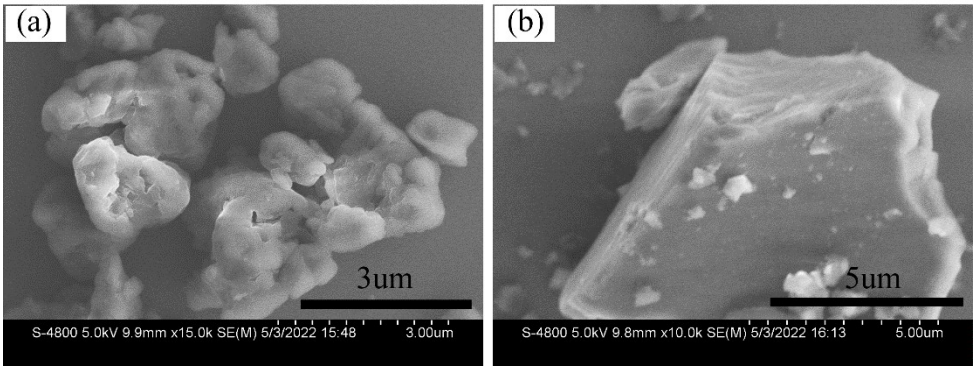

Fig. S5. SEM image of (a) o-CTF and (b) CTF.

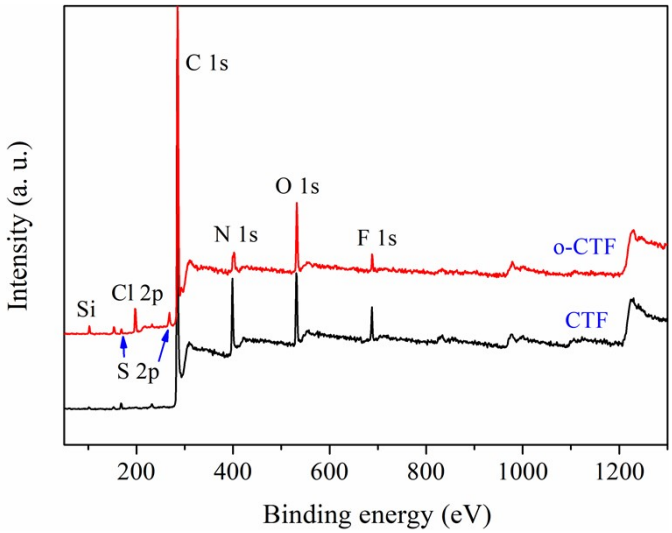

Fig. S6. XPS survey of CTF and o-CTF.

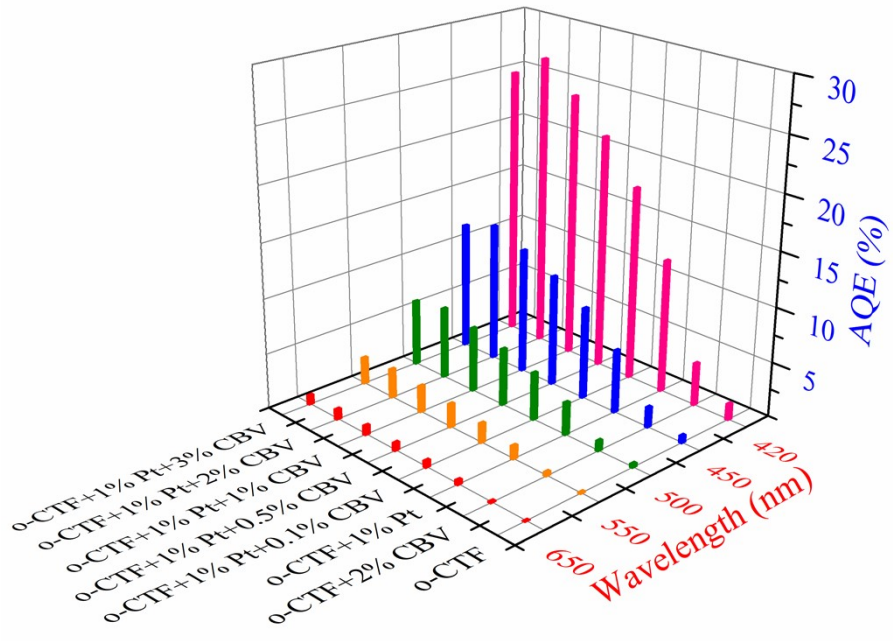

Fig. S7. Apparent quantum efficiency (AQE) of o-CTF for photocatalytic hydrogen evolution coupled with different amount CBV.

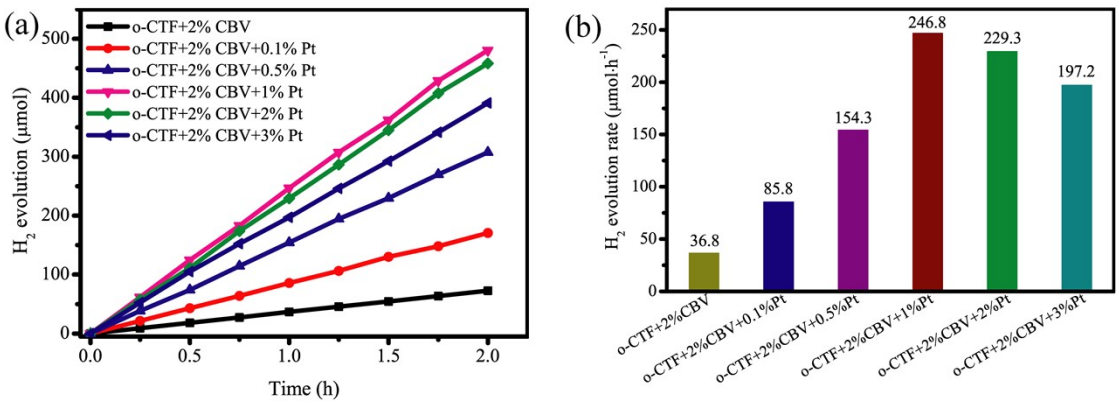

Fig. S8. (a) Photocatalytic H_2 evolution tests and (b) H_2 evolution rate comparison of o-CTF+2%CBV with different amount Pt co-catalyst.

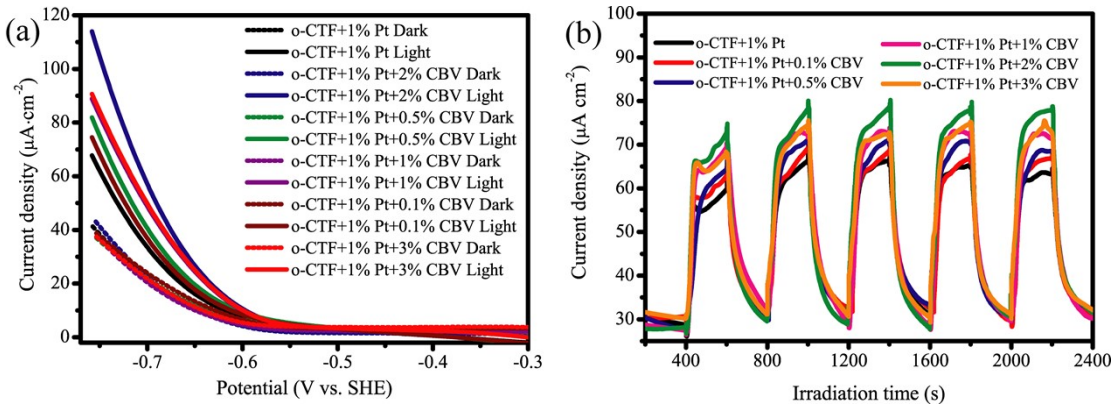

Fig. S9. (a) LSV curves of o-CTF+1%Pt coupled with different amount CBV. (b) Photocurrent measurements of o-CTF+1%Pt coupled with different amount CBV at -0.7 V (vs. SHE). Measurements were conducted in 0.2 mol·L^{-1} Na_2SO_4 solution under 300W Xenon lamp irradiation.

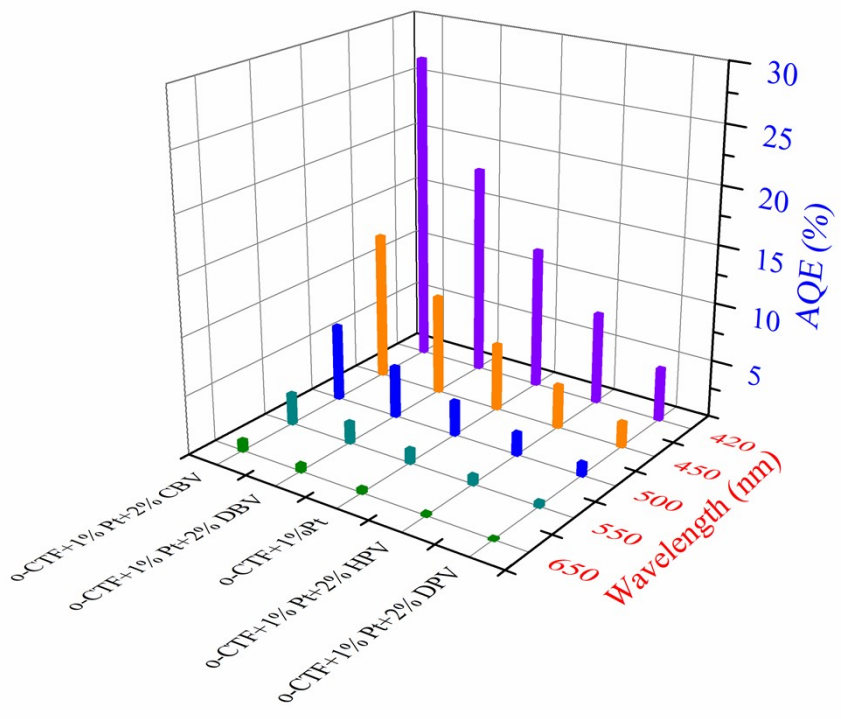

Fig. S10. Apparent quantum efficiency (AQE) of o-CTF+1%Pt for photocatalytic hydrogen evolution coupled with 2 wt.% CBV, DBV, DPV and HPV.

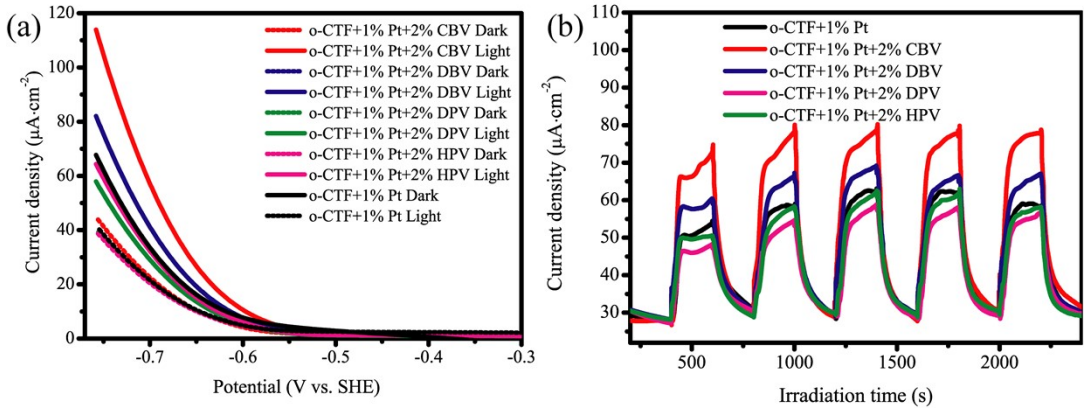

Fig. S11. (a) LSV curves of o-CTF+1%Pt coupled with 2 wt.% CBV, DBV, DPV and HPV. (b) Photocurrent measurements of o-CTF+1%Pt coupled with 2 wt.% CBV, DBV, DPV and HPV at -0.7 V (vs. SHE). Measurements are conducted in 0.2 mol·L^{-1} Na_2SO_4 solution under Xenon lamp irradiation.

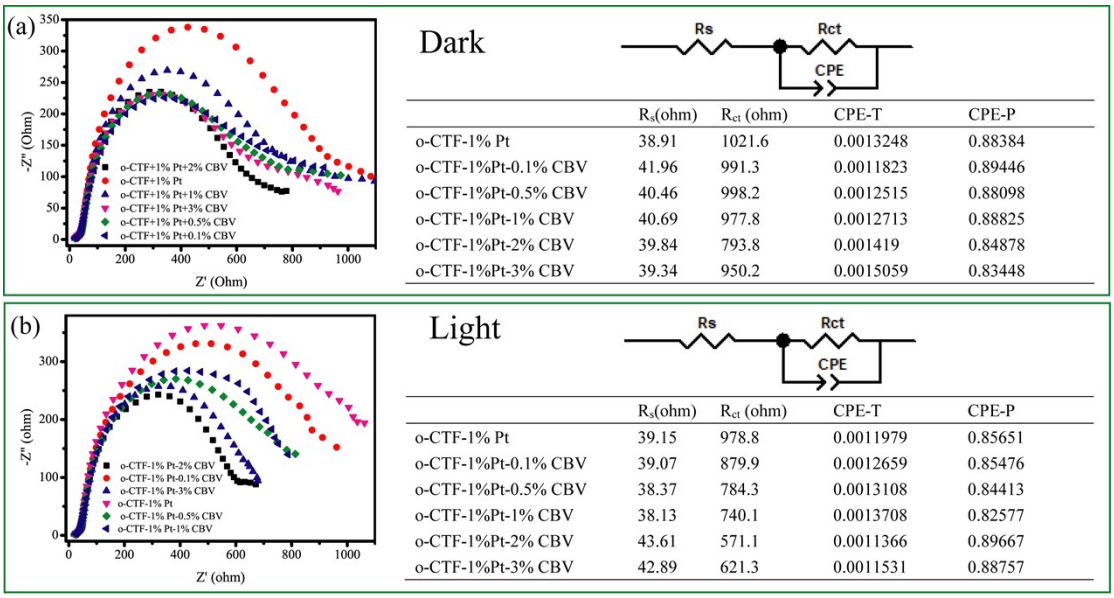

	R_s(ohm)	R_{ct} (ohm)	CPE-T	CPE-P
o-CTF-1% Pt	38.91	1021.6	0.0013248	0.88384
o-CTF-1%Pt-0.1% CBV	41.96	991.3	0.0011823	0.89446
o-CTF-1%Pt-0.5% CBV	40.46	998.2	0.0012515	0.88098
o-CTF-1%Pt-1% CBV	40.69	977.8	0.0012713	0.88825
o-CTF-1%Pt-2% CBV	39.84	793.8	0.001419	0.84878
o-CTF-1%Pt-3% CBV	39.34	950.2	0.0015059	0.83448

	R_s(ohm)	R_{ct} (ohm)	CPE-T	CPE-P
o-CTF-1% Pt	39.15	978.8	0.0011979	0.85651
o-CTF-1%Pt-0.1% CBV	39.07	879.9	0.0012659	0.85476
o-CTF-1%Pt-0.5% CBV	38.37	784.3	0.0013108	0.84413
o-CTF-1%Pt-1% CBV	38.13	740.1	0.0013708	0.82577
o-CTF-1%Pt-2% CBV	43.61	571.1	0.0011366	0.89667
o-CTF-1%Pt-3% CBV	42.89	621.3	0.0011531	0.88757

Fig. S12. Nyquist plots, equivalent circuits and the fitting results of impedance spectrum of o-CTF+1%Pt mixed with different amount CBV under (a) dark and (b) light condition. Measurements were conducted in 0.2 mol L^{-1} Na_2SO_4 solution containing CBV molecule with different concentrations.

Additional discussion: CPE referred to constant phase element in circuit.

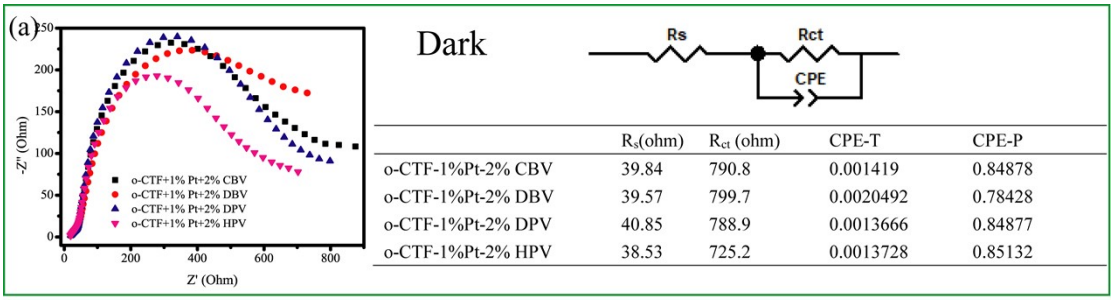

	R_s(ohm)	R_{ct} (ohm)	CPE-T	CPE-P
o-CTF-1%Pt-2% CBV	39.84	790.8	0.001419	0.84878
o-CTF-1%Pt-2% DBV	39.57	799.7	0.0020492	0.78428
o-CTF-1%Pt-2% DPV	40.85	788.9	0.0013666	0.84877
o-CTF-1%Pt-2% HPV	38.53	725.2	0.0013728	0.85132

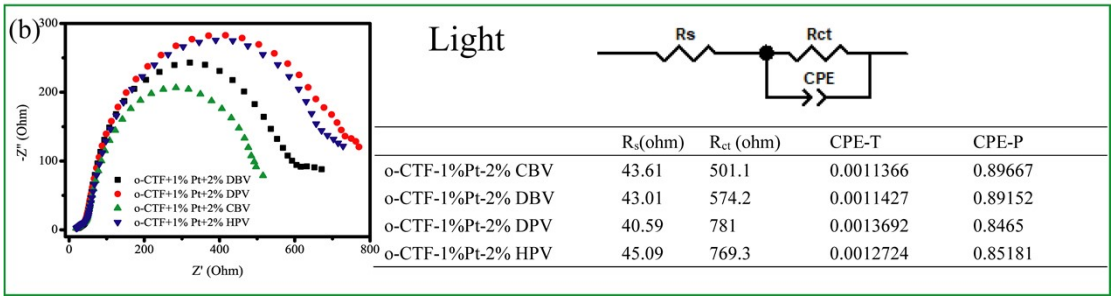

	R_s(ohm)	R_{ct} (ohm)	CPE-T	CPE-P
o-CTF-1%Pt-2% CBV	43.61	501.1	0.0011366	0.89667
o-CTF-1%Pt-2% DBV	43.01	574.2	0.0011427	0.89152
o-CTF-1%Pt-2% DPV	40.59	781	0.0013692	0.8465
o-CTF-1%Pt-2% HPV	45.09	769.3	0.0012724	0.85181

Fig. S13. Nyquist plots, equivalent circuits and the fitting results of impedance spectrum of o-CTF+1% Pt mixed with 2 wt. % CBV, DBV, DPV and HPV under (a) dark and (b) light condition. Measurements were conducted in 0.2 mol L^{-1} Na_2SO_4 solution containing 2 wt. % CBV, DBV, DPV and HPV, respectively.

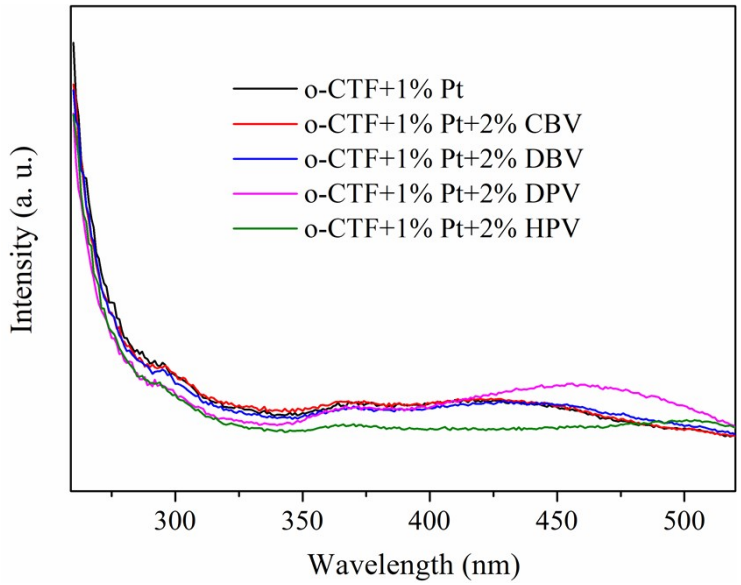

Fig. S14. Photoluminescence excitation spectra of o-CTF, mixed with 1 wt.% Pt and 2 wt.% CBV, DBV, DPV and HPV, measured at 610 nm.

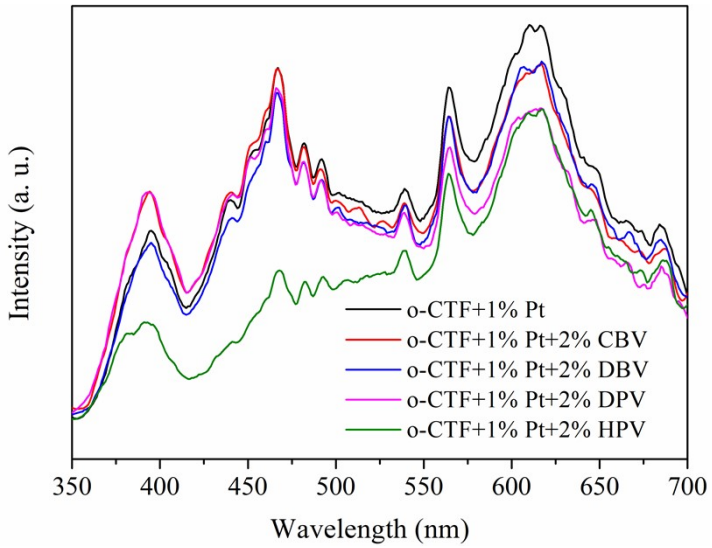

Fig. S15. Photoluminescence emission spectra of o-CTF mixed with 1 wt.% Pt and 2 wt.% CBV, DBV, DPV and HPV. The excitation wavelength was 270 nm.

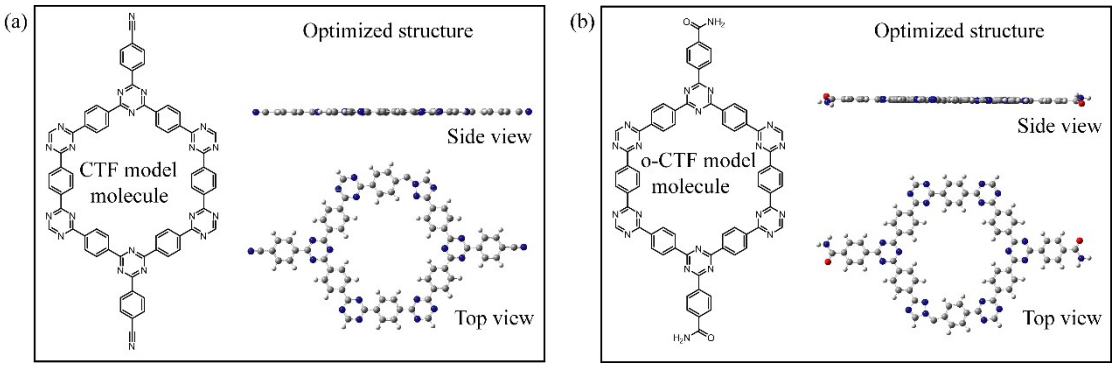

Fig. S16. The model molecule of (a) CTF and (b) o-CTF, and the corresponding top

and side view of the optimized structures.

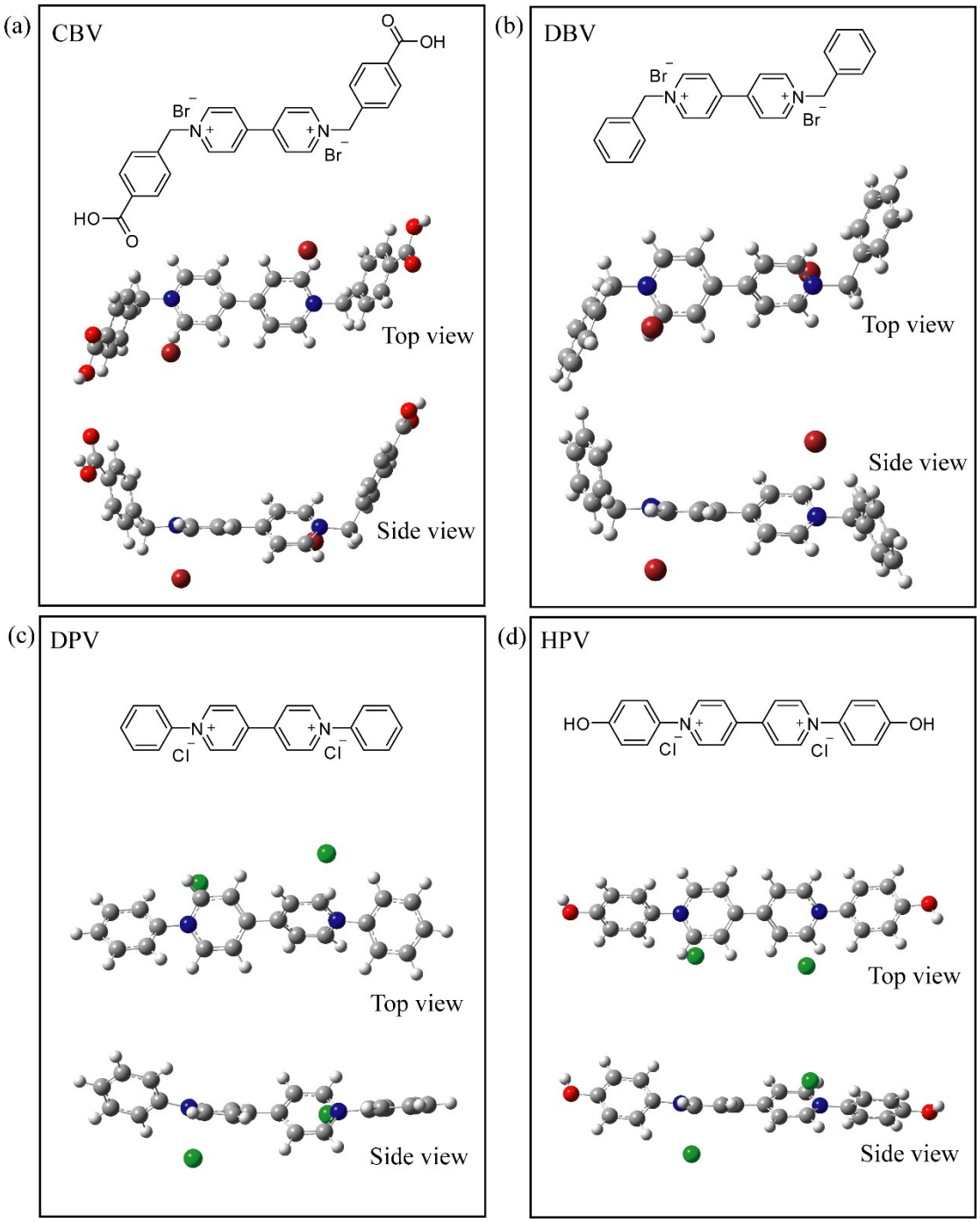

Fig. S17. The top and side view of the optimized structures for (a) CBV, (b) DBV, (c) DPV and (d) HPV.

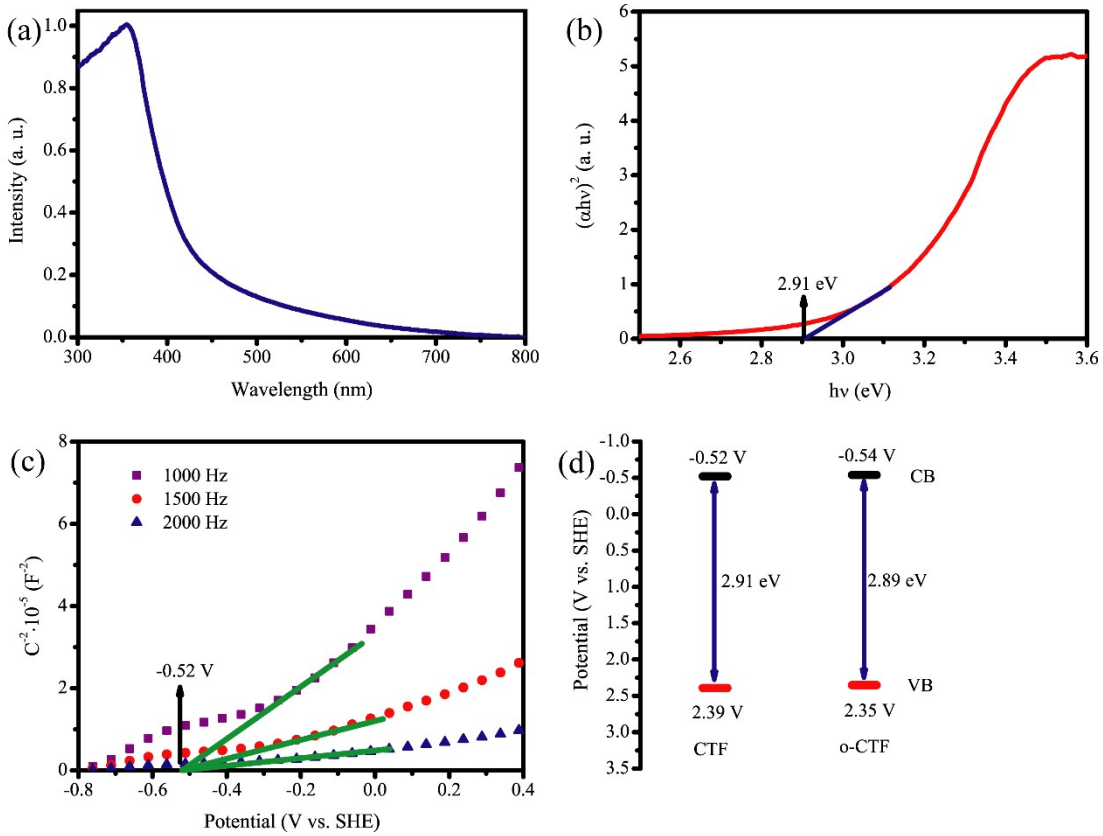

Fig. S18. (a) Ultraviolet–visible diffuse reflectance spectrum of CTF. (b) Kubelka–Munk plots converted from the UV–vis diffuse reflectance spectrum of CTF. (c) Mott-Schottky plots of CTF. (d) Band structure diagram comparison of CTF and o-CTF.

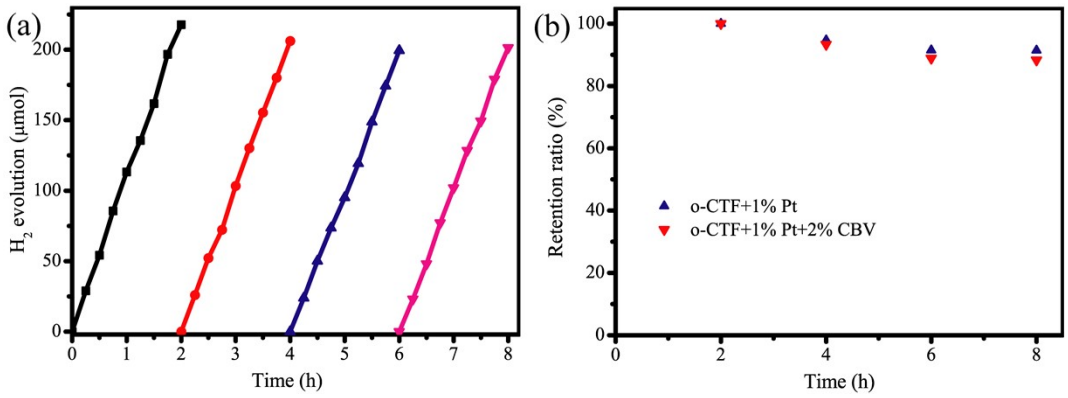

Fig. S19. (a) Photostability test of o-CTF+1%Pt for photocatalytic H_2 evolution. (b) Photostability comparison of o-CTF+1%Pt and o-CTF+1%Pt+2%CBV.

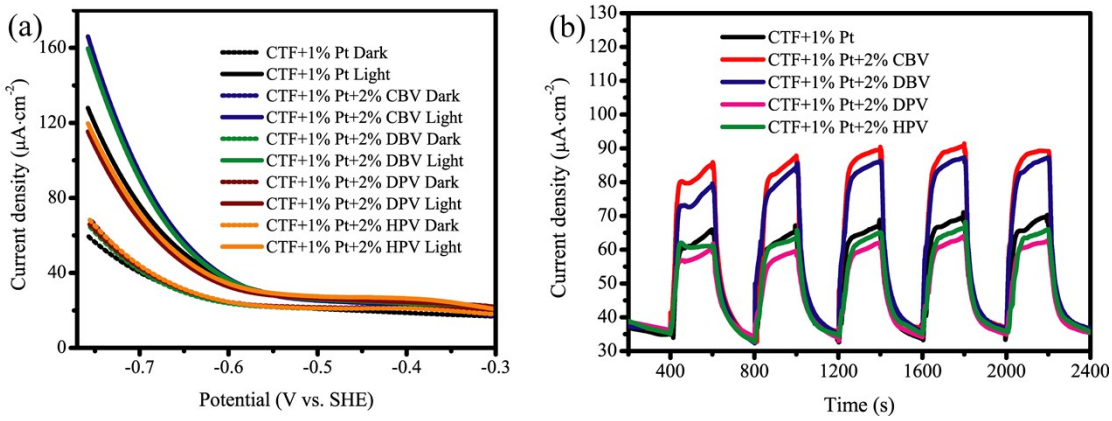

Fig. S20. (a) LSV curves of CTF+1%Pt coupled with 2 wt. % CBV, DBV, DPV and HPV. (b) Photocurrent measurements of CTF+1%Pt coupled with 2 wt. % CBV, DBV, DPV and HPV at -0.7 V (vs. SHE). Measurements were conducted in 0.2 mol·L^{-1} Na_2SO_4 solution under Xenon lamp irradiation.

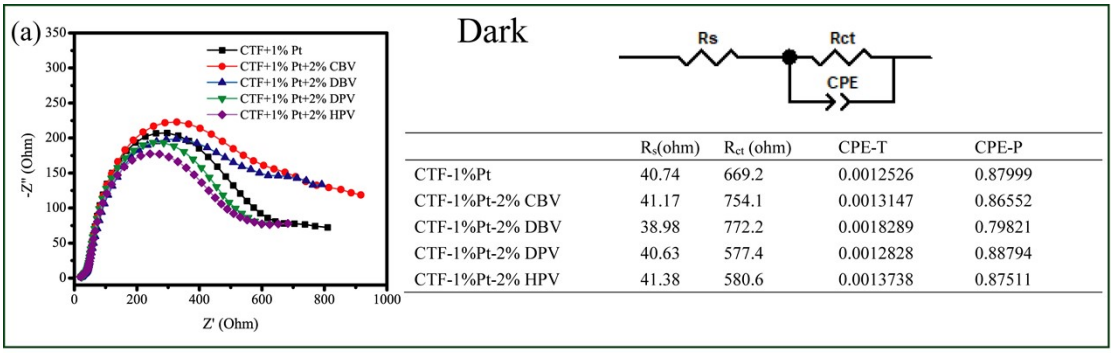

	R_s(ohm)	R_{ct} (ohm)	CPE-T	CPE-P
CTF-1%Pt	40.74	669.2	0.0012526	0.87999
CTF-1%Pt-2% CBV	41.17	754.1	0.0013147	0.86552
CTF-1%Pt-2% DBV	38.98	772.2	0.0018289	0.79821
CTF-1%Pt-2% DPV	40.63	577.4	0.0012828	0.88794
CTF-1%Pt-2% HPV	41.38	580.6	0.0013738	0.87511

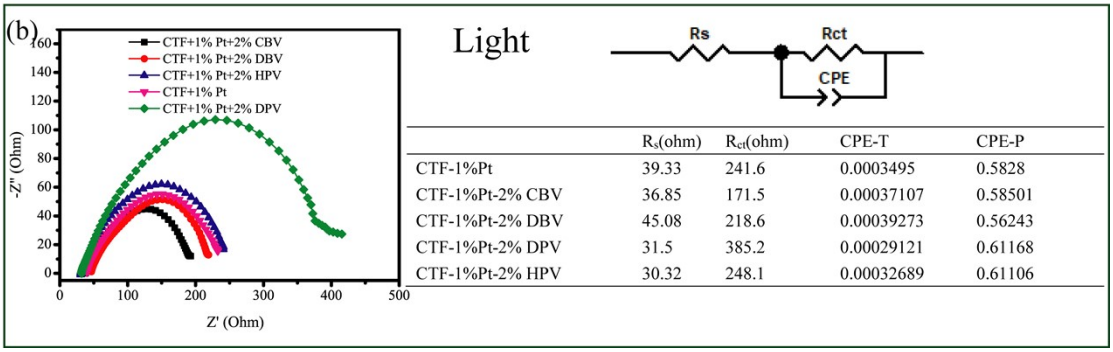

	R_s(ohm)	R_{ct}(ohm)	CPE-T	CPE-P
CTF-1%Pt	39.33	241.6	0.0003495	0.5828
CTF-1%Pt-2% CBV	36.85	171.5	0.00037107	0.58501
CTF-1%Pt-2% DBV	45.08	218.6	0.00039273	0.56243
CTF-1%Pt-2% DPV	31.5	385.2	0.00029121	0.61168
CTF-1%Pt-2% HPV	30.32	248.1	0.00032689	0.61106

Fig. S21. Nyquist plots, equivalent circuits and the fitting results of impedance spectrum of CTF+1%Pt mixed with 2 wt.% CBV, DBV, DPV and HPV under (a) dark and (b) light condition. Measurements were conducted in 0.2 mol L^{-1} Na_2SO_4 solution containing 2 wt.% CBV, DBV, DPV and HPV, respectively.

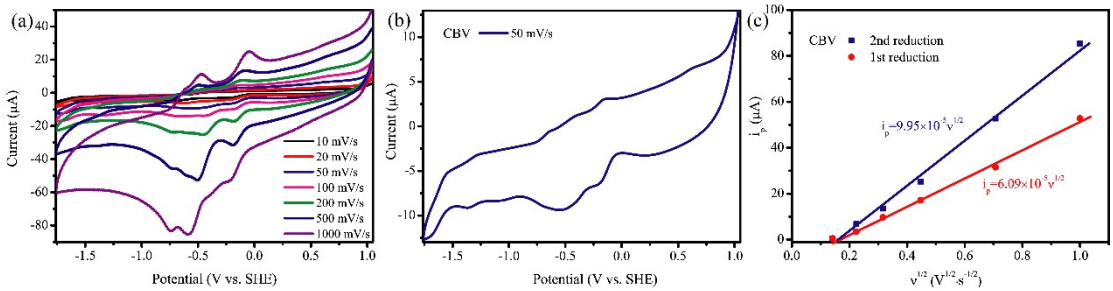

Fig. S22. The cyclic voltammogram (CV) of CBV (a) at different scan speeds and (b) at 50 mV/s in DMSO solution using tetrabutylammonium hexafluorophosphate (0.05 mol L^{-1}) as supporting electrolyte. (c) Peak current and scan speed diagram of CBV according to Nicholson's formula by the analysis with cyclic voltammetry in Fig. S22a.

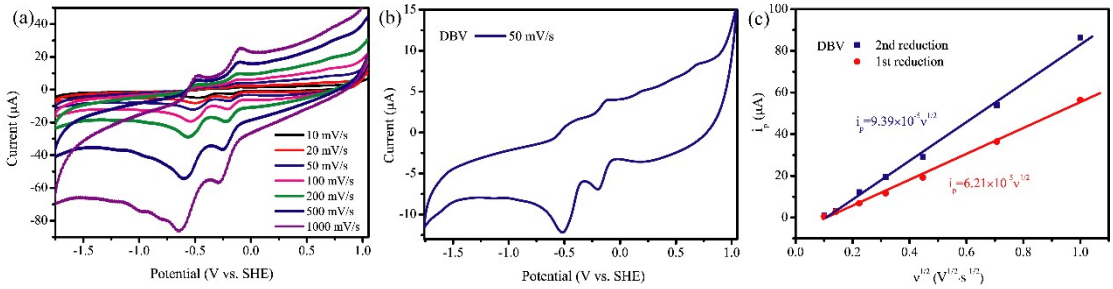

Fig. S23. The cyclic voltammogram (CV) of DBV (a) at different scan speeds and (b) at 50 mV/s in DMSO solution using tetrabutylammonium hexafluorophosphate (0.05 mol L^{-1}) as supporting electrolyte. (c) Peak current and scan speed diagram of DBV according to Nicholson's formula by the analysis with cyclic voltammetry in Fig. S23a.

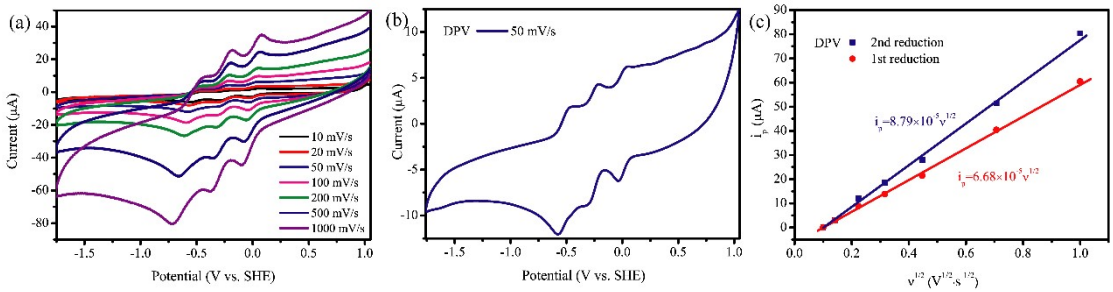

Fig. S24. The cyclic voltammogram (CV) of DPV (a) at different scan speeds and (b) at 50 mV/s in DMSO solution using tetrabutylammonium hexafluorophosphate (0.05 mol L^{-1}) as supporting electrolyte. (c) Peak current and scan speed diagram of DPV

according to Nicholson's formula by the analysis with cyclic voltammetry in Fig. S24a.

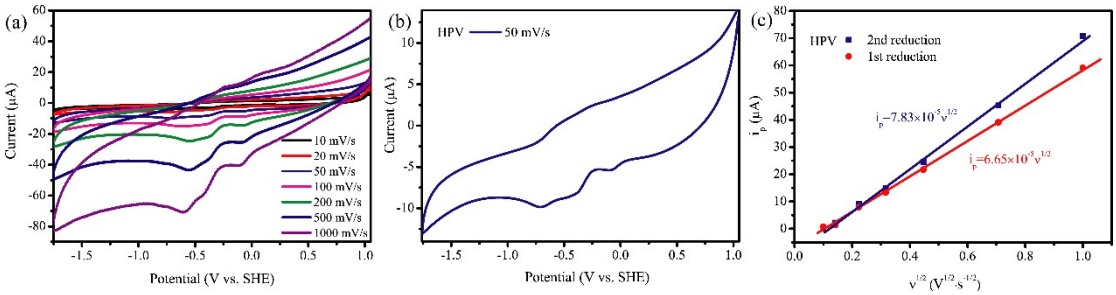

Fig. S25. The cyclic voltammogram (CV) of HPV (a) at different scan speeds and (b) at 50 mV/s in DMSO solution using tetrabutylammonium hexafluorophosphate (0.05 mol L^{-1}) as supporting electrolyte. (c) Peak current and scan speed diagram of HPV according to Nicholson's formula by the analysis with cyclic voltammetry in Fig. S25a.

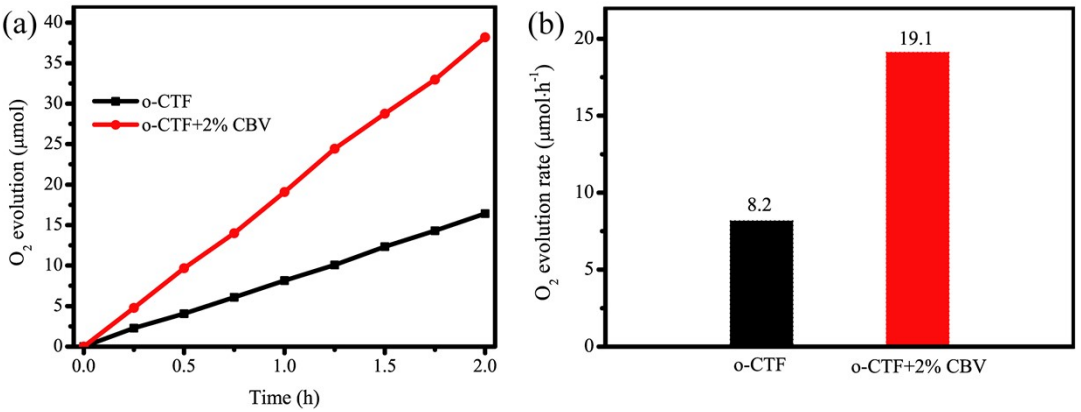

Fig. S26. (a) Photocatalytic O_2 evolution tests and (b) O_2 evolution rate comparison of o-CTF and o-CTF+2%CBV.

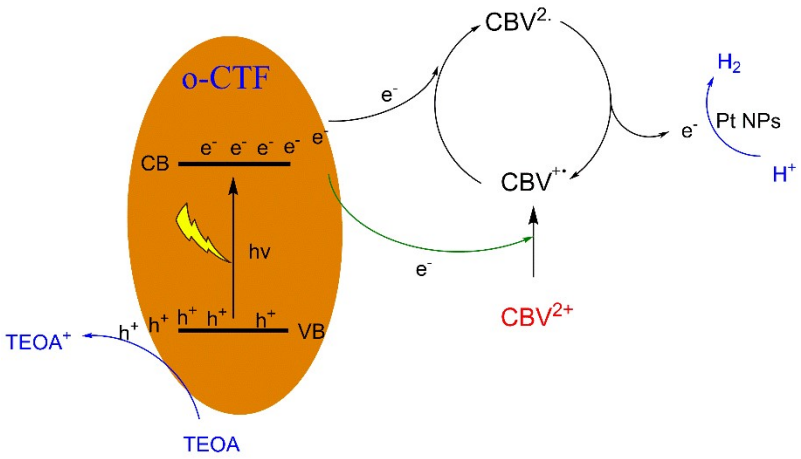

Fig. S27. The electron transferred pathway in photocatalytic HER process under o-CTF+1%Pt+2%CBV catalyzing.

Additional discussion: Initially, CBV^{2+} was reduced to $CBV^{+\cdot}$ by one electron came from o-CTF CB. Then, $CBV^{+\cdot}$ was further reduced to $CBV^{2\cdot}$ by another electron came from o-CTF CB. The $CBV^{2\cdot}$ would donate one electron to proton for proton reducing. At the same time, $CBV^{2\cdot}$ was re-oxidized to $CBV^{+\cdot}$ species. Immediately, $CBV^{+\cdot}$ was re-reduced to $CBV^{2\cdot}$ by electrons came from o-CTF CB and $CBV^{2\cdot}$ continued to reduce proton for hydrogen evolution. Thus, the catalytic cycle was triggered.

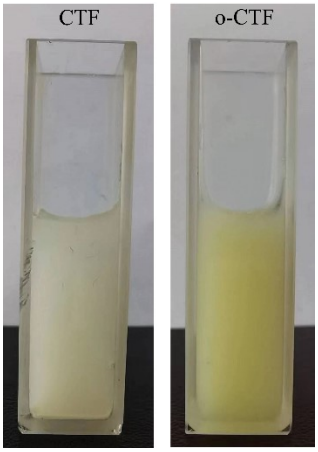

Fig. S28. The photographs of CTF and o-CTF dispersion (10 mg/mL) in water after naturally lay up for 30 minutes.

Additional discussion: 30 mg CTF and o-CTF were dispersed into 3 mL deionized water, respectively. The suspensions were then sonicated for 30 min for uniform

dispersion. And then, the suspensions were naturally lay up for 30 minutes for photographs colecting. Obviously, the o-CTF suspension was still uniform dispersed in water without any precipitation. However, part of CTF powder deposited at the bottom after naturally lay up for 30 minutes due to its large size.

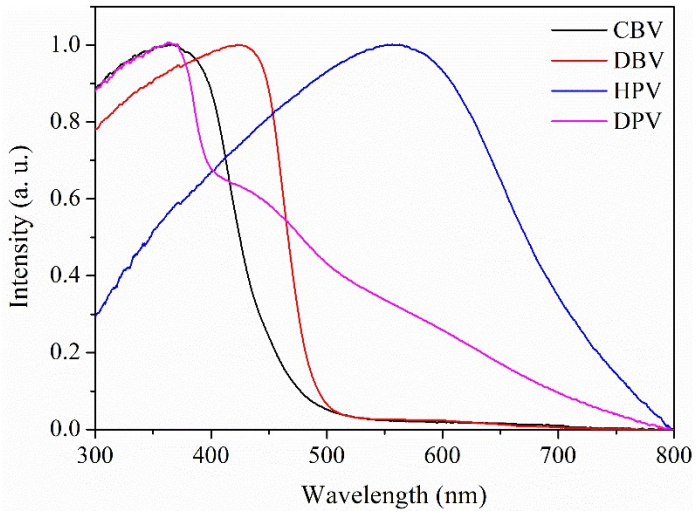

Fig. S29. UV-vis diffuse reflextion speatra of CBV, DBV, DPV and HPV.

Additional discussion: Compared to the UV-Vis DRS of o-CTF+1%Pt in Fig. 4b and the UV-Vis DRS of viologen derivatives in Fig. S29, the UV-Vis DRS of o-CTF+1%Pt mixed with 2 wt.% viologen derivatives, including o-CTF+1%Pt+2%CBV, o-CTF+1%Pt+2%DBV, o-CTF+1%Pt+2%DPV, o-CTF+1%Pt+2%HPV, were simple stack of UV-Vis DRS from o-CTF+1%Pt and viologen derivatives.

Table S1. The fitted parameters of time-resolved transient photoluminescence decay spectra.

Samples	B_1	B_2	B_2	τ_1 (ns)	τ_2 (ns)	τ_3 (ns)	$\bar{\tau}$ (ns)
o-CTF+1%Pt	4.76	0.067	0.023	8.26	134.58	744.90	218.4
o-CTF+1%Pt+2%CBV	0.138	0.047	0.015	27.40	186.95	882.68	520.5

o-CTF+1%Pt+2%DBV	0.071	0.049	0.024	34.28	170.80	729.19	504.3
o-CTF+1%Pt+2%DPV	3.763	0.041	0.013	5.48	123.65	623.51	171.4
o-CTF+1%Pt+2%HPV	0.356	0.064	0.013	17.44	118.91	531.78	226.2

Table S2. Atomic content in CTF and o-CTF originated from theoretical calculation, XPS survey and elemental analysis (EA).

	Calculated (wt.%)			XPS (wt.%)			EA (wt.%)		
	C	N	H	C	N	O	C	N	H
CTF	74.99	21.86	3.15	80.06	12.20	7.58	68.21	18.29	3.90
o-CTF	-	-	-	76.26	14.00	7.22	64.00	17.61	3.45

Table S3. The calculated N atomic content (wt.%), originated from –C=N-, -C≡N and -$CONH_2$ configuration, according to the N 1s XPS deconvolution of CTF and o-CTF.

	-C=N-	-C≡N	-$CONH_2$
CTF	10.32	1.88	0
o-CTF	5.88	0.61	7.51

Table S4. The calculated C atomic content (wt.%), originated from –C=N-, -C=C and -$CONH_2$ configuration, according to the C 1s XPS deconvolution of CTF and o-CTF.

	-C=N-	-C=C	-$CONH_2$
CTF	7.53	72.53	0
o-CTF	0	63.37	12.89

Table S5. The evaluated electron-transfer constant k_{ET} by the Nicholson's formula.

Entry	CBV		DBV		DPV		HPV	
	1st red	2nd red	1st red	2nd red	1st red	2nd red	1st red	2nd red
slope of fitted $i_p \sim \upsilon^{\frac{1}{2}}$ curve	6.09×10^{-5}	9.95×10^{-5}	6.21×10^{-5}	9.39×10^{-5}	6.68×10^{-5}	8.79×10^{-5}	6.65×10^{-5}	7.83×10^{-5}

$D^{1/2}$	3.23×10^{-3}	5.28×10^{-3}	3.30×10^{-3}	4.99×10^{-3}	3.55×10^{-3}	4.67×10^{-3}	3.53×10^{-3}	4.16×10^{-3}
Ψ	7	0.8	1	1	0.7	0.6	0.7	0.5
k_{ET}**(cm s^{-1})**	10.6×10^{-3}	1.98×10^{-3}	1.55×10^{-3}	2.34×10^{-3}	1.16×10^{-3}	1.31×10^{-3}	1.15×10^{-3}	0.98×10^{-3}

Table S6. The comparison of photocatalytic hydrogen evolution rate and AQE over reported CTF photocatalysts.

Photocatalyst	**Light source**	**Sacrificial reagent**	**HER rate (μmol h^{-1} g^{-1})**	**AQE (%)**	**References**
r-CTF NSs/3%Pt	300 W Xe-lamp (λ > 420 nm)	TEOA	10200	11.3 (420 nm)	S1
BP/CTF	300 W Xe-lamp (λ > 420 nm)	Formaldehyde	17100	31.6 (420 nm)	S5
Cl-ECF/3%Pt	300 W Xe-lamp (λ > 420 nm)	Lactic acid	1300	N/A	S6
CTF-HUST-2/3%Pt	300 W Xe-lamp (λ > 420 nm)	TEOA	2647	N/A	S7
CTF-HUST-C1/3%Pt	300 W Xe-lamp (λ > 420 nm)	TEOA	5100	N/A	S8
CTF-02-$Bpy_{0.66}$/5%Pt	200 W Xe-lamp (λ > 396 nm)	TEOA	7240	1.6 (420 nm)	S9
CTF-$HS_{0.75}$-2/3%Pt	300 W Xe-lamp (λ > 420 nm)	TEOA	6040	4.2 (420 nm)	S10
CTF-ES_T/3%Pt	300 W Xe-lamp (λ > 420 nm)	TEOA	2000	4.6 (420 nm)	S11
CTF-BT/Th-1/3%Pt	300 W Xe-lamp (λ > 420 nm)	TEOA	6600	7.3 (420 nm)	S12
CTF-BP-Pt/2%Pt	300 W Xe-lamp (λ > 400 nm)	TEOA	614.5	N/A	S13
CTF-N/1%Pd	300 W Xe-lamp	TEOA	10556	N/A	S14

	(λ > 420 nm)				
CTFs/3%Pt	300 W Xe-lamp (λ > 420 nm)	TEOA	7971	N/A	S15
CTF-HUST-A1/3%Pt	300 W Xe-lamp (λ > 420 nm)	TEOA	9200	7.4 (420 nm)	S16
CTF-0/3%Pt	300 W Xe-lamp (λ > 420 nm)	TEOA	7010	8.0 (420 nm)	S17
CTF-N/3%Pt	300 W Xe-lamp (λ > 420 nm)	TEOA	10760	4.11 (420 nm)	S18
o-CTF/1%Pt/2%CBV	300 W Xe-lamp (λ > 420 nm)	TEOA	24680	26.9 (420 nm)	This work

References

[S1] C. X. Wang, H. L. Zhang, W. J. Luo, T. Sun, Y. X. Xu, *Angew. Chem. Int. Ed.*, 2021, ***60***, 25381-25390.

[S2] M. M. Cetin, Y. Beldjoudi, I. Roy, O. Anamimoghadam, Y. J. Bae, R. M. Young, M. D. Krzyaniak, C. L. Stern, D. Philp, F. M. Alsubaie, M. R. Wasielewski, J. F. Stoddart, *J. Am. Chem. Soc.*, 2019, ***141***, 18727−18739.

[S3] O. Buyukcakir, S. H. Je, S. N. Talapaneni, D. Kim, A. Coskun, *ACS Appl. Mater. Interfaces*, 2017, ***9***, 7209−7216.

[S4] R. S. Nicholson, *Anal. Chem.*, 1965, ***37***, 1351-1355.

[S5] L. W. Zhang, Y. M. Zhang, X. J. Huang, L. M. Tao, Y. P. Bi, *Appl. Catal. B: Environ.*, 2021, ***283***, 119633.

[S6] S. Li, M. F. Wu, T. Guo, L. L. Zheng, D. K. Wang, Y. Mu, Q. J. Xing, J. P. Zou, *Appl. Catal. B Environ.*, 2020, ***272***, 118989.

[S7] K. W. Wang, L. M. Yang, X. Wang, L. P Guo, G. Cheng, C. Zhang, S. B. Jin, B. E. Tan, A. Cooper, *Angew. Chem. Int. Ed.*, 2017, ***56***, 14149-14153.

[S8] M. Y. Liu, Q. Huang, S. L. Wang, Z. Y. Li, B. Y. Li, S. B. Jin, B. E. Tan, *Angew. Chem. Int. Ed.*, 2018, ***57***, 11968-11972.

[S9] M. A. Fávaro, D. Ditz, J. Yang, S. Bergwinkl, A. C. Ghosh, M. Stammler, C. Lorentz, J. Roeser, E. A. Quadrelli, A. Thomas, R. Palkovits, J. Canivet, F. M. Wisser, *ACS Appl. Mater. Interfaces*, 2022, ***14***, 14182-14192.

[S10] N. Wang, G. Cheng, L. P. Guo, B. E. Tan, S. B. Jin, *Adv. Funct. Mater.*, 2019, ***29***, 1904781.

[S11] Z. A. Lan, M. Wu, Z. P. Fang, Y. F. Zhang, X. Chen, G. G. Zhang, X. C. Wang, *Angew. Chem. Int. Ed.*, 2022, ***61***, e202201482.

[S12] W. Huang, Q. He, Y. P. Hu, Y. G. Li, *Angew. Chem. Int. Ed.*, 2019, ***58***, 8676-8680.

[S13] L. L. Zheng, D. K. Wang, S. L. Wu, X. H. Jiang, J. Zhang, Q. J. Xing, J. P. Zou, S. L. Luo, *J. Mater. Chem. A*, 2020, ***8***, 25425-25430.

[S14] M. Y. Liu, X. Q. Wang, J. Liu, K. W. Wang, S. B. Jin, B. E. Tan, *ACS Appl. Mater. Interfaces*, 2020, ***12***, 12774-12782.

[S15] T. Sun, Y. Liang, Y. X. Xu, *Angew. Chem. Int. Ed.*, 2022, ***61***, e202113926.

[S16] S. Q. Zhang, G. Cheng, L. P. Guo, N. Wang, B. E. Tan, S. B. Jin, *Angew. Chem. Int. Ed.*, 2020, ***59***, 6007-6014.

[S17] D. Kong, X. Y. Han, J. J. Xie, Q. S. Ruan, C. D. Windle, S. Windle, K. Shen, Z. M. Bai, Z. X. Guo, J. W. Tang, *ACS. Catal.*, 2019, ***9***, 7697-7707.

[S18] L. P. Guo, Y. L. Niu, H. T. Xu, Q. W. Li, S. Razzaque, Q. Huang, S. B. Jin, B. E. Tan, *J. Mater. Chem. A*, 2018, ***6***, 19775-19781.